



Conserved Eukaryotic Fusogens Can Fuse Viral Envelopes to Cells

Ori Avinoam *et al.*
Science **332**, 589 (2011);
DOI: 10.1126/science.1202333

This copy is for your personal, non-commercial use only.

If you wish to distribute this article to others, you can order high-quality copies for your colleagues, clients, or customers by [clicking here](#).

Permission to republish or repurpose articles or portions of articles can be obtained by following the guidelines [here](#).

The following resources related to this article are available online at www.sciencemag.org (this information is current as of July 22, 2014):

Updated information and services, including high-resolution figures, can be found in the online version of this article at:

<http://www.sciencemag.org/content/332/6029/589.full.html>

Supporting Online Material can be found at:

<http://www.sciencemag.org/content/suppl/2011/03/22/science.1202333.DC1.html>

This article **cites 18 articles**, 6 of which can be accessed free:

<http://www.sciencemag.org/content/332/6029/589.full.html#ref-list-1>

This article has been **cited by** 4 articles hosted by HighWire Press; see:

<http://www.sciencemag.org/content/332/6029/589.full.html#related-urls>

This article appears in the following **subject collections**:

Cell Biology

http://www.sciencemag.org/cgi/collection/cell_biol

ulations, which would otherwise be impossible with an intrinsic activation mechanism alone. We observe that regenerative hair patterns can differ in the same animal under different physiological conditions, allowing organisms to adapt to the environment (e.g., pregnancy in mice) (12). At the evolutionary scale, macroenvironmental regulation makes hair growth a trait that has high modularity. Lastly, beyond HFs, the experimental accessibility of this system offers a model for analyzing the fundamental principles of self-organizing behaviors in biological systems composed of coupled cycling elements.

References and Notes

- E. Fuchs, *Cell Stem Cell* **4**, 499 (2009).
- L. Li, H. Clevers, *Science* **327**, 542 (2010).
- C.-M. Chuong, M. K. Richardson, *Int. J. Dev. Biol.* **53**, 653 (2009).
- T. X. Jiang, H. S. Jung, R. B. Widellitz, C. M. Chuong, *Development* **126**, 4997 (1999).
- S. Sick, S. Reinker, J. Timmer, T. Schlake, *Science* **314**, 1447 (2006); 10.1126/science.1130088.
- K. S. Stenn, R. Paus, *Physiol. Rev.* **81**, 449 (2001).
- R. J. Morris *et al.*, *Nat. Biotechnol.* **22**, 411 (2004).
- N. Suzuki, M. Hirata, S. Kondo, *Proc. Natl. Acad. Sci. U.S.A.* **100**, 9680 (2003).
- M. V. Plikus, C.-M. Chuong, *J. Invest. Dermatol.* **128**, 1071 (2008).
- Materials and methods are available as supporting material on Science Online.
- S. Wolfram, *A New Kind of Science* (Wolfram Media, Champaign, IL, 2002).
- M. V. Plikus *et al.*, *Nature* **451**, 340 (2008).
- S. Reddy *et al.*, *Mech. Dev.* **107**, 69 (2001).
- D. Enshell-Seiffers, C. Lindon, M. Kashiwagi, B. A. Morgan, *Dev. Cell* **18**, 633 (2010).
- H. J. Whiteley, *Nature* **181**, 850 (1958).
- M. Cutrone, R. Grimalt, *Eur. J. Pediatr.* **164**, 630 (2005).
- J. Halloy, B. A. Bernard, G. Lousouarn, A. Goldbeter, *Proc. Natl. Acad. Sci. U.S.A.* **97**, 8328 (2000).
- R. J. Antaya, E. Sideridou, E. A. Olsen, *J. Am. Acad. Dermatol.* **53** (suppl. 1), S130 (2005).

Acknowledgments: C.-M.C. is supported by National Institute of Arthritis and Musculoskeletal and Skin Diseases RO1-AR42177, AR60306, and AR47364; S.E.M. by RO1-AR47709; R.E.B. by a UK Engineering and Physical Sciences Research Council First grant; P.K.M. by a Royal Society Wolfson Research Merit Award; and M.V.P. by a California Institute for Regenerative Medicine postdoctoral grant. There is a USC patent application partially based on the work in this study on the compositions and methods to modulate hair growth.

Supporting Online Material

www.sciencemag.org/cgi/content/full/332/6029/586/DC1
Materials and Methods
Figs. S1 to S16
Tables S1 to S3
Movies S1 to S9

14 December 2010; accepted 25 March 2011
10.1126/science.1201647

Conserved Eukaryotic Fusogens Can Fuse Viral Envelopes to Cells

Ori Avinoam,¹ Karen Fridman,¹ Clari Valansi,¹ Inbal Abutbul,² Tzviya Zeev-Ben-Mordehai,³ Ulrike E. Maurer,⁴ Amir Sapir,^{1*} Dganit Danino,² Kay Grünewald,^{3,4} Judith M. White,⁵ Benjamin Podbilewicz^{1†}

Caenorhabditis elegans proteins AFF-1 and EFF-1 [C. *elegans* fusion family (CeFF) proteins] are essential for developmental cell-to-cell fusion and can merge insect cells. To study the structure and function of AFF-1, we constructed vesicular stomatitis virus (VSV) displaying AFF-1 on the viral envelope, substituting the native fusogen VSV glycoprotein. Electron microscopy and tomography revealed that AFF-1 formed distinct supercomplexes resembling pentameric and hexameric “flowers” on pseudoviruses. Viruses carrying AFF-1 infected mammalian cells only when CeFFs were on the target cell surface. Furthermore, we identified fusion family (FF) proteins within and beyond nematodes, and divergent members from the human parasitic nematode *Trichinella spiralis* and the chordate *Branchiostoma floridae* could also fuse mammalian cells. Thus, FF proteins are part of an ancient family of cellular fusogens that can promote fusion when expressed on a viral particle.

Membrane fusion is critical for many biological processes such as fertilization, development, intracellular trafficking, and viral infection (1–6). Current models of the molecular mechanisms of membrane fusion rely on experimental and biophysical analyses performed on viral and intracellular, minimal, fusion-mediating machineries. Yet, how well these models correspond to the mechanisms of cell-cell

fusion is unknown (4, 5). *Caenorhabditis elegans* fusion family (CeFF) proteins were identified as C. *elegans* fusogens that are expressed at the time and place of cell fusion in vivo (7, 8). Expression of CeFF proteins is essential for developmental cell fusion via hemifusion and sufficient to fuse cells in vivo and in insect cell cultures (8–10).

To identify putative fusion family (FF) members in other species, we conducted sequence comparisons (4, 11). These comparisons yielded putative members in 35 nematodes, two arthropods (*Calanus finmarchicus* and *Lepeophtheirus salmonis*), a ctenophore (*Pleurobrachia pileus*), a chordate (*Branchiostoma floridae*), and a protist (*Naegleria gruberi*) (Fig. 1A). FF proteins are putative members of the “mostly β sheet super family” and share a pattern of cysteines, implying that they are conserved at the level of structure (fig. S1).

To determine whether divergent FF proteins maintained their function as fusogens through evolution, we expressed FF proteins from the human parasitic nematode *Trichinella spiralis*

(*Tsp-ff-1*) and the chordate *B. floridae* (*Bfl-ff-1*) in baby hamster kidney (BHK) cells and compared their fusogenic activity to AFF-1 (Fig. 1, B to F). These orthologs share 26 and 22% sequence identity with AFF-1, respectively. We observed, by immunofluorescence, $28 \pm 4\%$ and $37 \pm 7\%$ multinucleation in cells transfected with *Tsp-ff-1* and *Bfl-ff-1*, compared with $26 \pm 2\%$ and $4 \pm 3\%$ multinucleation in controls transfected with *aff-1* and empty vector, respectively (Fig. 1F) (11). In addition, when we expressed the EFF-1 paralog from the nematode *Pristionchus pacificus* in C. *elegans* embryos, we detected ectopic fusion of cells that normally do not fuse (fig. S2). Thus, FF proteins represent a conserved family of cellular fusogens.

To explore whether FF proteins can functionally substitute for viral fusogens, we complemented VSV Δ G pseudoviruses with AFF-1 (Fig. 2 and fig. S3). We initially used a recombinant vesicular stomatitis virus (VSV) called VSV Δ G, in which the glycoprotein G (VSVG) gene was replaced by a green fluorescent protein (GFP) reporter, to infect BHK cells overexpressing VSVG (11–16). The resulting VSV Δ G-G viruses were capable of only a single round of infection, manifested by the production of GFP. We achieved complementation with AFF-1 by VSV Δ G-G infection of BHK cells expressing AFF-1 (BHK–AFF-1), which generated pseudotyped particles carrying the nematode fusogen (VSV Δ G–AFF-1). We biochemically validated incorporation of AFF-1 into VSV Δ G pseudotypes by SDS–polyacrylamide gel electrophoresis, Coomassie staining, silver staining, immunoblotting, and mass spectrometry (11). We found that the major proteins on VSV Δ G–AFF-1 were the viral proteins N, P, L, M, and AFF-1. For comparison, we also analyzed VSV Δ G-G and VSV Δ G (fig. S4 and table S5). Infection of BHK–AFF-1 cells with VSV Δ G–AFF-1 showed a 600-fold increase compared with infection of BHK control cells not expressing AFF-1 (Fig. 2A). Although infection due to residual VSVG-complemented VSV Δ G (VSV Δ G-G) was negli-

¹Department of Biology, Technion–Israel Institute of Technology, Haifa 32000, Israel. ²Department of Biotechnology and Food Engineering and The Russell Berrie Nanotechnology Institute, Technion–Israel Institute of Technology, Haifa 32000, Israel. ³Oxford Particle Imaging Centre, Division of Structural Biology, Wellcome Trust Centre for Human Genetics, University of Oxford, Oxford, OX3 7BN, UK. ⁴Department of Molecular Structural Biology, Max-Planck Institute of Biochemistry, D-82152 Martinsried, Germany. ⁵Department of Cell Biology, University of Virginia, Charlottesville, VA 22908, USA.

*Present address: Howard Hughes Medical Institute and Division of Biology, California Institute of Technology, Pasadena, CA 91125, USA.

†To whom correspondence should be addressed. E-mail: podbilew@technion.ac.il

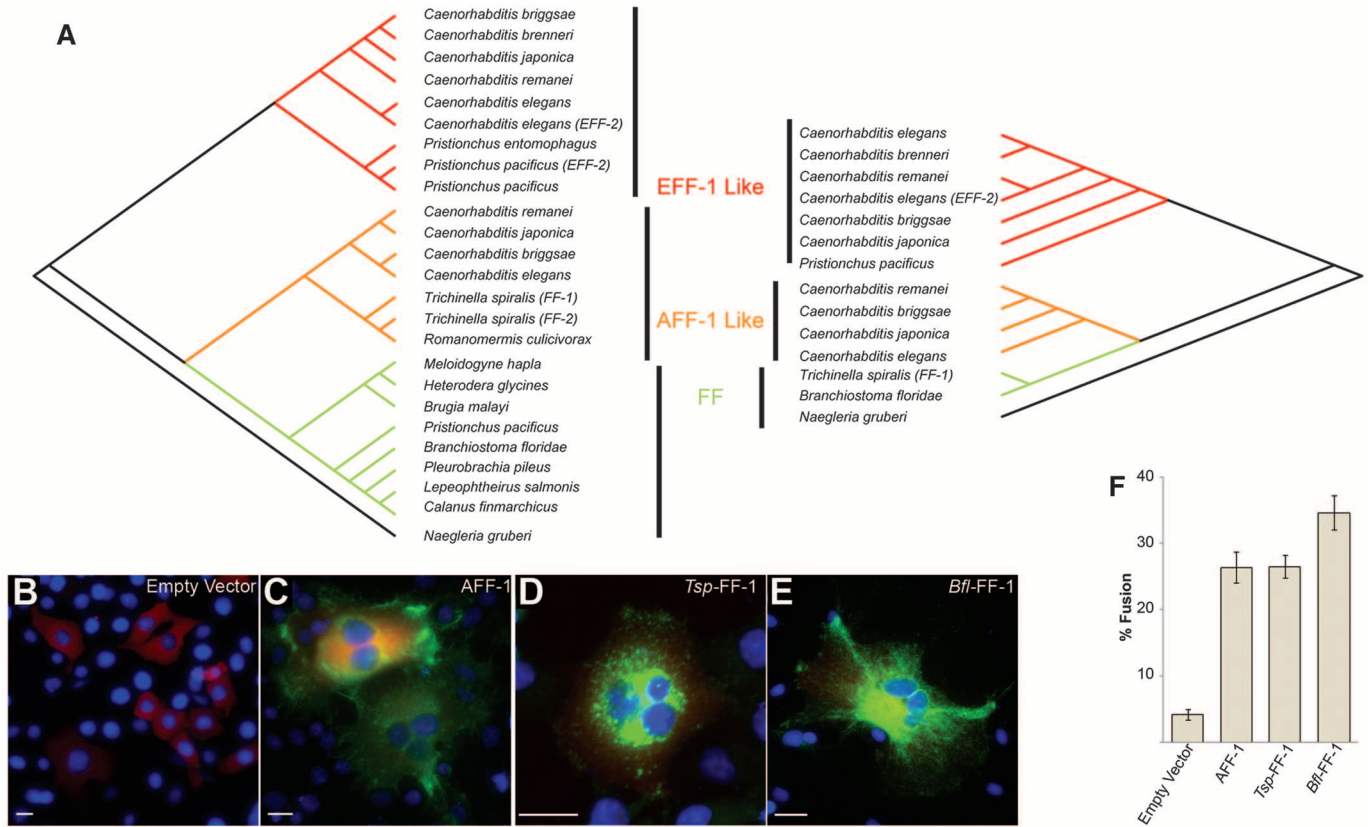


Fig. 1. A family of eukaryotic cell-cell fusogens: FF orthologs from two phyla fuse mammalian BHK cells. (A) Two trees produced using maximum parsimony analysis show phylogenetic relationships of 25 taxa [(left) based on the transforming growth factor- β -receptor type I-like domain (fig. S1B)] and 14 taxa [(right) based on the full-length extracellular domain]; FF proteins are classified into three subgroups: EFF-1-like (red), AFF-1-like (orange), and FF (green) (table S1). Consistency, retention, and composite indexes are detailed in (11). (B

to E) Immunofluorescence with anti-Flag antibodies (green) and nuclei 4',6-diamidino-2-phenylindole staining (blue) on BHK cells transfected with (B) empty vector, (C) *aff-1*, (D) *Tsp-ff-1*, and (E) *Bfl-ff-1*. Cotransfection marker is shown in red. Scale bars, 20 μ m. (F) Fusion index for BHKs expressing FF proteins and negative control (empty vector). Data are means \pm SE (error bars). Empty vector, $n = 14$; *aff-1*, $n = 14$; *Tsp-ff-1*, $n = 8$; *Bfl-ff-1*, $n = 9$ (n represents the number of experiments).

gible (Fig. 2), we performed inoculations in the presence of a neutralizing monoclonal antibody to G (anti-G antibody mAb 11) (17) to assure that we only measured AFF-1-mediated infection (fig. S5). Thus, AFF-1 can replace the viral fusogen VSVG and can mediate virus-to-cell binding and fusion.

VSV Δ G-AFF-1 could also infect cells expressing EFF-1 (BHK-EFF-1) (Fig. 2A) with comparable efficiency, suggesting that different CeFF proteins can functionally interact to mediate membrane fusion. To test this hypothesis, we evaluated cytoplasmic mixing between cells. We coexpressed *aff-1* with a red fluorescent protein containing a nuclear export signal (RFPnes) (Fig. 3) and mixed them with cells coexpressing *eff-1* and a cyan fluorescent protein containing a nuclear localization signal (CFPnl) (18). We cocultured the two cell populations and observed multinucleated cells expressing both markers (Fig. 3). In contrast, we did not observe cells that were cotransfected with empty vector (Fig. 3A). Thus, AFF-1 and EFF-1 can promote heterotypic membrane fusion. To show independently that these results were a consequence of fusion, we recorded

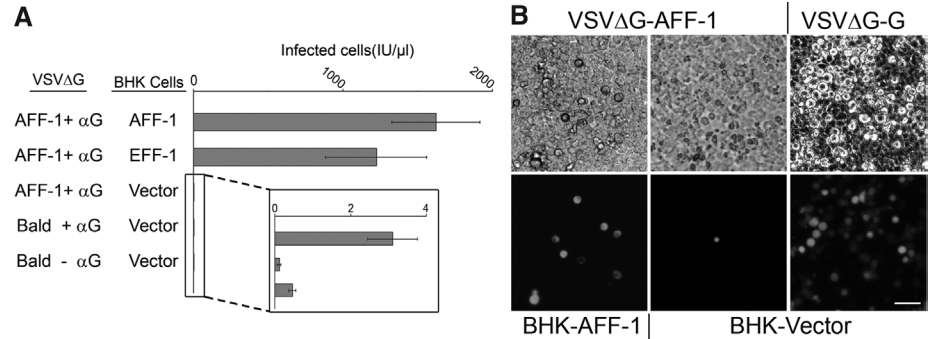


Fig. 2. AFF-1 can complement the infection of a fusion-deficient VSV Δ G. (A) Titers of VSV Δ G pseudoviruses. The type of protein on the viral membrane (bald or AFF-1) and on the BHK cell membrane (vector, AFF-1, or EFF-1) is indicated (fig. S3). Anti-VSVG antibody (α G) was used to neutralize any residual VSV Δ G-G virus (fig. S5) (11). Titers are measured in infectious units (IU), representing the number of cells expressing GFP per microliter 24 hours after virus inoculation. Data are mean \pm SE (error bars; $n = 3$ experiments). (Inset) Background infection. We found no significant difference between infection of BHK-AFF-1 and BHK-EFF-1 (two-tailed paired t test, $P = 0.5841$). (B) Infection of BHKs monitored as GFP expression. (Top) phase contrast; (bottom) fluorescence. VSV Δ G-G served as positive control (fig. S5). Scale bar, 50 μ m.

time-lapse images of BHK-AFF-1 cells (fig. S6 and movies S1 and S2), supporting the conclusion that AFF-1 expression was enough to fuse cells.

Hence, AFF-1 and EFF-1 can mediate cell-cell fusion as well as viral-cell fusion by a CeFF-mediated mechanism. However, the VSV Δ G-

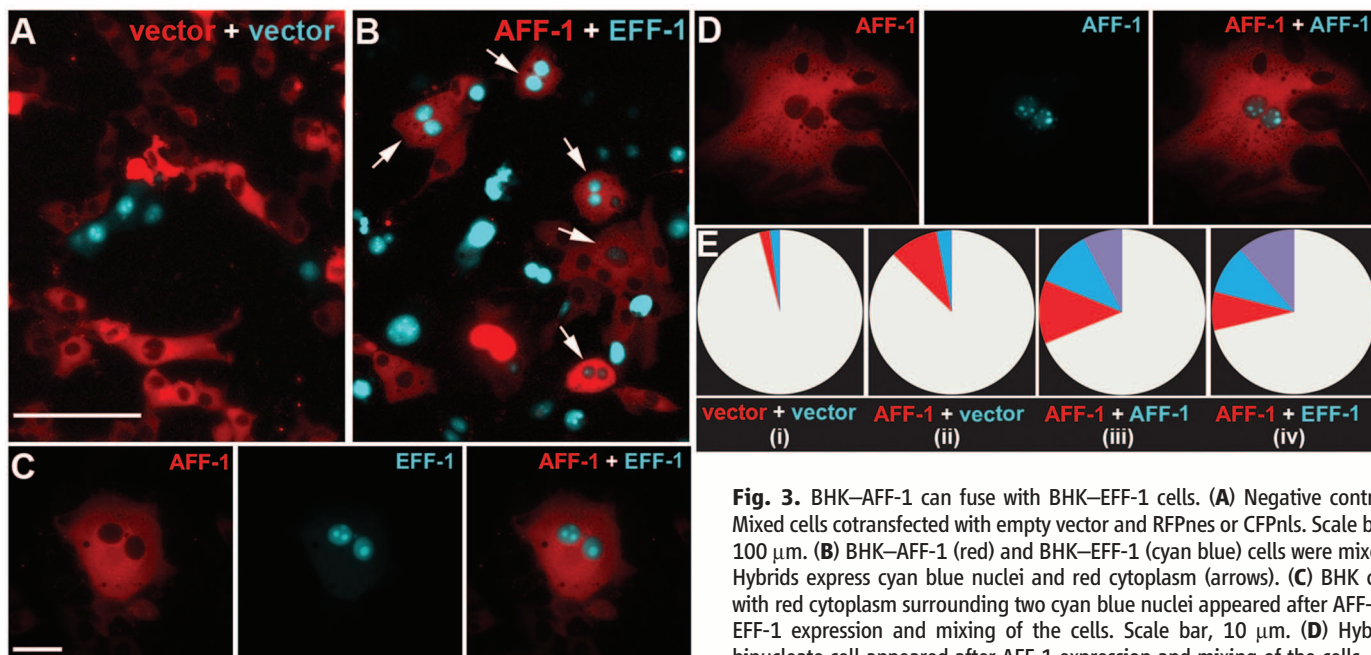


Fig. 3. BHK–AFF-1 can fuse with BHK–EFF-1 cells. **(A)** Negative control. Mixed cells cotransfected with empty vector and RFPnes or CFPnls. Scale bar, 100 μ m. **(B)** BHK–AFF-1 (red) and BHK–EFF-1 (cyan blue) cells were mixed. Hybrids express cyan blue nuclei and red cytoplasm (arrows). **(C)** BHK cell with red cytoplasm surrounding two cyan blue nuclei appeared after AFF-1–EFF-1 expression and mixing of the cells. Scale bar, 10 μ m. **(D)** Hybrid binucleate cell appeared after AFF-1 expression and mixing of the cells. **(E)**

Quantification of content mixing experiments. Red, cyan blue, and purple pie sections represent the fraction of multinucleated cells (two nuclei or higher). Results are mean of four independent experiments ($n \geq 1000$ total cells). (i) Empty vector transfected cells only. All multinucleated cells were binucleated (red or cyan blue, not purple); total binucleate cells = 4%, probably dividing cells. (ii) AFF-1–expressing cells (red) mixed with empty vector transfected cells (cyan blue). Elevation in multinucleation was only observed for AFF-1–expressing cells (red, 11%; cyan blue, 3%). One cell with a single nucleus expressing both markers (red and cyan blue) was observed. (iii) AFF-1–expressing cells (red) mixed with AFF-1–expressing cells (cyan blue), resulting in four cell populations: mononucleated (white, 64%), multinucleated (red, 13%; cyan blue, 12%), and mixed (purple, 11%). (iv) AFF-1–expressing cells (red, 9%) mixed with EFF-1–expressing cells (cyan blue, 11%). AFF-1– and EFF-1–expressing cells fuse (purple, 18%).

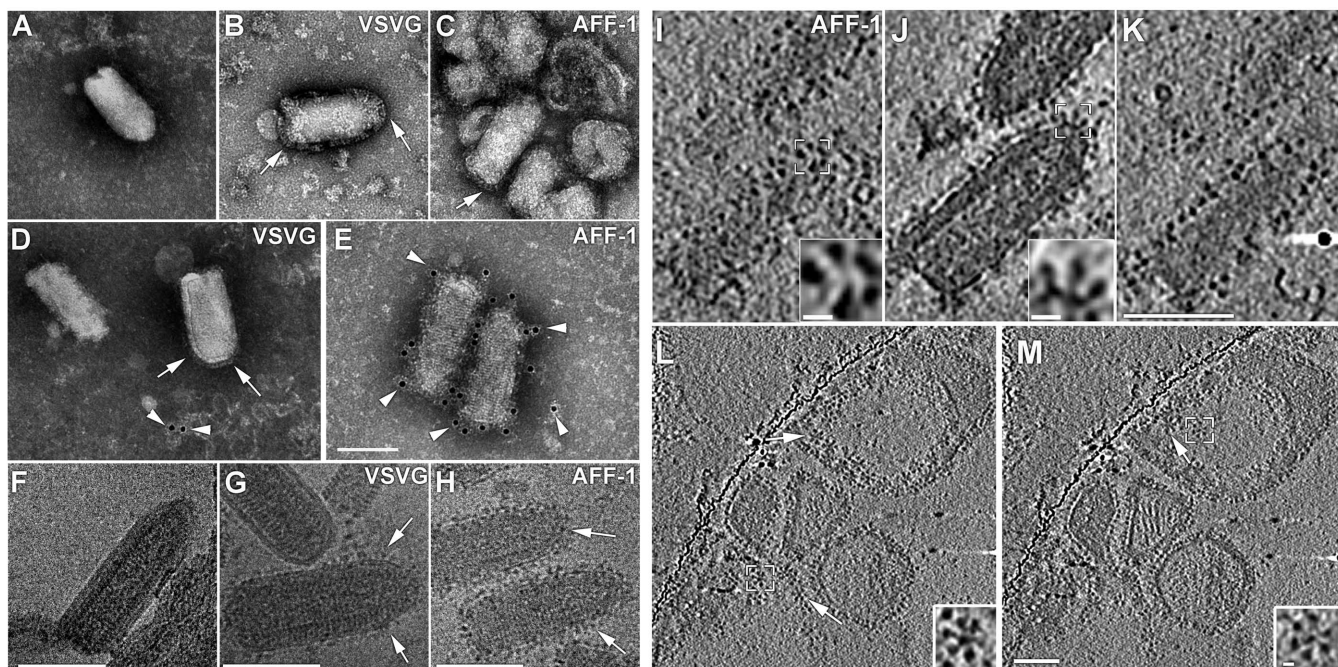


Fig. 4. EM of VSV Δ G–AFF-1 reveals specific bulky surface spikes. **(A to C)** Negative-stained particles of **(A)** VSV Δ G, **(B)** VSV Δ G–G, and **(C)** VSV Δ G–AFF-1. **(D and E)** Anti–AFF-1 polyclonal antibodies followed by immunogold labeling and negative stain of **(D)** VSV Δ G–G and **(E)** VSV Δ G–AFF-1 (figs. S7 and S8). **(F to H)** Cryo-EM of **(F)** VSV Δ G, **(G)** VSV Δ G–G, and **(H)** VSV Δ G–AFF-1. **(I to K)** Top, center, and bottom slice, respectively, from

VSV Δ G–AFF-1 tomogram (movie S3). **(L and M)** Slices from cryo-ET of vesicles copurified with VSV Δ G–AFF-1 preparations displaying penta- or hexameric flower-shaped assemblies (movie S5). Scale bars, 100 nm (main panels); 10 nm (insets). Arrows, surface spike assemblies; arrowheads, gold particles. The white squares in **(I)**, **(J)**, **(L)**, and **(M)** indicate the areas shown magnified in the insets.

AFF-1 infection mechanism is fundamentally different from that of native VSV. Whereas the infection of VSV is mediated by VSVG only on the viral membrane, infection mediated by VSVΔG–AFF-1 requires an FF protein on both the viral membrane and the cell membrane.

To study the relation between structure and function of AFF-1, we used transmission electron microscopy (TEM). We compared negatively stained samples of VSVΔG to VSVG- and AFF-1-complemented VSVΔG preparations (11). VSVΔG virions have the typical VSV shape with a smooth membrane (hence, they are termed “bald”), whereas both VSVΔG-G (19) and VSVΔG–AFF-1 virions displayed distinct spikes on their envelopes (Fig. 4, A to C). In negative stain (pH 5), VSVG forms elongated spikes on VSVΔG-G (Fig. 4B) (19), whereas VSVΔG–AFF-1 showed shorter spikes (Fig. 4C). The estimated average spike lengths of VSVG and AFF-1 were 145 and 109 Å, respectively (table S2). To confirm that the observed spikes were indeed AFF-1, we used anti-AFF-1 polyclonal antibodies to perform immunogold labeling. We observed specific immunoreactivity on the surface of VSVΔG–AFF-1 (Fig. 4, D and E, and figs. S7 and S8). To further characterize the pseudoviruses at higher resolution and in a more native state, we used cryogenic TEM (cryo-TEM) (Fig. 4, F to H) and cryogenic electron tomography (cryo-ET) (Fig. 4, I to K, and movie S3) to image them embedded in vitreous ice. Cryo-TEM projection images showed that AFF-1 proteins coat the pseudoviruses. Side views of individual spikes could be observed at central sections of the tomograms

(Fig. 4J). Higher-order assemblies of AFF-1 in the form of penta- or hexameric “flower-shaped” supercomplexes could be observed in slices through the tomogram oriented peripheral to the pseudotyped virus particles (Fig. 4I). These assemblies were more visible in slices through the tomograms of copurified vesicles (Fig. 4, L and M, fig. S9, and movies S4 and S5). The order of these arrays may have a critical function in bending and deforming plasma membranes to mediate fusion.

Here, we have presented evidence that FF proteins are functionally conserved in evolution and can restore the infectivity of VSVΔG through interactions with FF proteins on the target cell. Thus, FF, viral, and intracellular fusogens converge functionally as minimal fusion machines that function on their own to promote fusion.

References and Notes

1. W. Wickner, R. Schekman, *Nat. Struct. Mol. Biol.* **15**, 658 (2008).
2. S. Martens, H. T. McMahon, *Nat. Rev. Mol. Cell Biol.* **9**, 543 (2008).
3. J. M. White, S. E. Delos, M. Brecher, K. Schornberg, *Crit. Rev. Biochem. Mol. Biol.* **43**, 189 (2008).
4. A. Sapir, O. Avinoam, B. Podbilewicz, L. V. Chernomordik, *Dev. Cell* **14**, 11 (2008).
5. M. Oren-Suissa, B. Podbilewicz, *Trends Cell Biol.* **17**, 537 (2007).
6. E. H. Chen, E. Grote, W. Mohler, A. Vignery, *FEBS Lett.* **581**, 2181 (2007).
7. W. A. Mohler *et al.*, *Dev. Cell* **2**, 355 (2002).
8. A. Sapir *et al.*, *Dev. Cell* **12**, 683 (2007).
9. B. Podbilewicz *et al.*, *Dev. Cell* **11**, 471 (2006).
10. G. Shemer *et al.*, *Curr. Biol.* **14**, 1587 (2004).
11. Materials and methods are available as supporting material on Science Online.

12. J. Závada, *J. Gen. Virol.* **15**, 183 (1972).
13. M. J. Schnell, L. Buonocore, E. Kretzschmar, E. Johnson, J. K. Rose, *Proc. Natl. Acad. Sci. U.S.A.* **93**, 11359 (1996).
14. A. Takada *et al.*, *Proc. Natl. Acad. Sci. U.S.A.* **94**, 14764 (1997).
15. Y. Matsuura *et al.*, *Virology* **286**, 263 (2001).
16. S. Fukushi *et al.*, *J. Gen. Virol.* **86**, 2269 (2005).
17. L. Lefrançois, D. S. Lyles, *Virology* **121**, 157 (1982).
18. C. Hu *et al.*, *Science* **300**, 1745 (2003).
19. S. Libersou *et al.*, *J. Cell Biol.* **191**, 199 (2010).

Acknowledgments: We thank I. Nagano, M. Whitt, A. Fire, C. Giraud, and J. Rothman for reagents; F. Glaser, M. Glickman, A. Harel, O. Kleinfeld, T. Schwartz, I. Sharon, E. Spooner, R. Sommer, and members of the White and Podbilewicz labs for discussions; the Smoler Proteomics Center at the Technion and the Whitehead Institute for Biomedical Research for mass spectrometry; T. Ziv for proteomics analysis; the Caenorhabditis Genetics Center for nematode strains; and I. Yanai and A. de Silva for critically reading the manuscript. This work was supported by grants from the FIRST Program of the Israel Science Foundation (ISF 1542/07 to B.P.), the Human Frontier Science Program (RG0079/2009-C to K.G.), and the NIH (AI22470 to J.M.W.), as well as a Wellcome Trust Senior Research Fellowship to K.G. The Technion Research and Development Foundation has filed a patent relating to methods and compositions useful in cell-cell fusion using FF proteins of nematode origin and to antinematodal methods and compositions, using proteins of the nematode fusion family.

Supporting Online Material

www.sciencemag.org/cgi/content/full/science.1202333/DC1
Materials and Methods
Figs. S1 to S9
Tables S1 to S5
References
Movies S1 to S5

29 December 2010; accepted 14 March 2011
Published online 24 March 2011;
10.1126/science.1202333

The Spatial Periodicity of Grid Cells Is Not Sustained During Reduced Theta Oscillations

Julie Koenig, Ashley N. Linder, Jill K. Leutgeb, Stefan Leutgeb*

Grid cells in parahippocampal cortices fire at vertices of a periodic triangular grid that spans the entire recording environment. Such precise neural computations in space have been proposed to emerge from equally precise temporal oscillations within cells or within the local neural circuitry. We found that grid-like firing patterns in the entorhinal cortex vanished when theta oscillations were reduced after intraseptal lidocaine infusions in rats. Other spatially modulated cells in the same cortical region and place cells in the hippocampus retained their spatial firing patterns to a larger extent during these periods without well-organized oscillatory neuronal activity. Precisely timed neural activity within single cells or local networks is thus required for periodic spatial firing but not for single place fields.

Brain oscillations are thought to be essential for neural computations and for organizing cognitive processes (1–5). Yet it has been difficult to distinguish computations in neural circuits that require oscillatory neural activity from those that occur irrespective of the precise temporal organization that oscillatory rhythms can

provide. Theta oscillations (4 to 11 Hz) can be recorded in the local field potential of the hippocampus and the parahippocampal cortices, including the entorhinal cortex. These brain regions are important for memory and navigation (6) and contain a number of different cell types with precise spatial firing patterns, such as place cells,

head-direction cells, and grid cells (7–9). Grid cells are found in the medial entorhinal cortex (MEC), parasubiculum, and presubiculum and have multiple firing peaks that form a highly regular hexagonal firing pattern in two-dimensional space (8, 10).

The coexistence of cells with well-defined spatial firing patterns and of theta oscillations that are particularly prominent during voluntary movement (11) suggests that oscillatory brain activity might be essential for spatial computations. In particular, it has been proposed that precisely tuned theta oscillations, as an animal moves through its environment, might be necessary for generating the periodic spatial firing of grid cells. Such spatial regularity might arise from interference between oscillators with small frequency differences, given that those oscillators are controlled by both movement velocity and movement direction (12–14). Although the oscillators could be implemented in various ways in single neurons or

Neurobiology Section and Center for Neural Circuits and Behavior, Division of Biological Sciences, University of California, San Diego, USA.

*To whom correspondence and requests for materials should be addressed. E-mail: sleutgeb@ucsd.edu